

5-27-2009

# On the Validity of the Top of the Barrier Quantum Transport Model for Ballistic Nanowire MOSFETs

Abhijeet Paul

*Purdue University - Main Campus*

Saumitra Mehrotra

*Purdue University - Main Campus*

Gerhard Klimeck

*Purdue University - Main Campus, gekco@purdue.edu*

Mathieu Luisier

*Purdue University - Main Campus*

---

Paul, Abhijeet; Mehrotra, Saumitra; Klimeck, Gerhard; and Luisier, Mathieu, "On the Validity of the Top of the Barrier Quantum Transport Model for Ballistic Nanowire MOSFETs" (2009). *Birck and NCN Publications*. Paper 426.

<http://docs.lib.purdue.edu/nanopub/426>

This document has been made available through Purdue e-Pubs, a service of the Purdue University Libraries. Please contact [epubs@purdue.edu](mailto:epubs@purdue.edu) for additional information.

# On the validity of the top of the barrier quantum transport model for ballistic nanowire MOSFETs

Abhijeet Paul, Saumitra Mehrotra, Gerhard Klimeck, and Mathieu Luisier

School of Electrical and Computer Engineering, Network for Computational Nanotechnology,  
and Birck Nanotechnology Center, Purdue University, West Lafayette, IN, USA - 47907

Email: [paul1@purdue.edu](mailto:paul1@purdue.edu)

**Abstract**— This work focuses on the determination of the valid device domain for the use of the Top of the barrier (ToB) model to simulate quantum transport in nanowire MOSFETs in the ballistic regime. The presence of a proper Source/Drain barrier in the device is an important criterion for the applicability of the model. Long channel devices can be accurately modeled under low and high drain bias with DIBL adjustment.

**Keywords**— component; nanowires; top of the barrier; MOSFET; ballistic transport model; DIBL; tunneling current; top-of-the-barrier; subthreshold- slope; Tight-Binding; Short channel effects .

## I. INTRODUCTION

Continuous shrinking of channel length ( $L_c$ ) in silicon CMOS devices to increase performance has led to the development of non-planar devices. Nanowire based Field-Effect-Transistors (FET) are an attractive candidate in this area due to better electrostatic gate control. Recently many experimental groups have demonstrated fabrication of silicon nanowire (SiNW) transistors of diameters even down to 3nm [1, 2, 3, 4, 5].

To understand the working of such small devices it is important to have proper theoretical model which encapsulates quantum transport mechanisms. A critical element in the model is the representation of the device in an atomistic Tight-Binding (TB) model [6], which understands the finite number of atoms in the structure, their local arrangement with details such as strain distribution and disorder [7, 8]. A full 3D atomistic quantum transport model [9, 10, 11] can provide the device characteristics, however, this model is computationally time consuming [12]. Recently, a 2D top of the barrier (ToB) atomistic quantum transport model [13, 14, 15] has been used for speedy simulation and analysis of SiNW FET device characteristics, which provides significant insight. However, to use the ToB model reliably, it is essential to understand the device regime where this model is valid.

In this work, the range of validity of 2D Top of the barrier atomistic quantum transport model is evaluated with a full 3D and atomistic model. Figure 1 shows that ToB inherently misses the channel length dependence; however, it can fetch accurate and fast results for long channel ballistic transistors. We observe a deviation in ToB vs. full 3D results as channel length is reduced. This difference is mostly attributed to the source/drain tunnelling current due to shrinking of the barrier

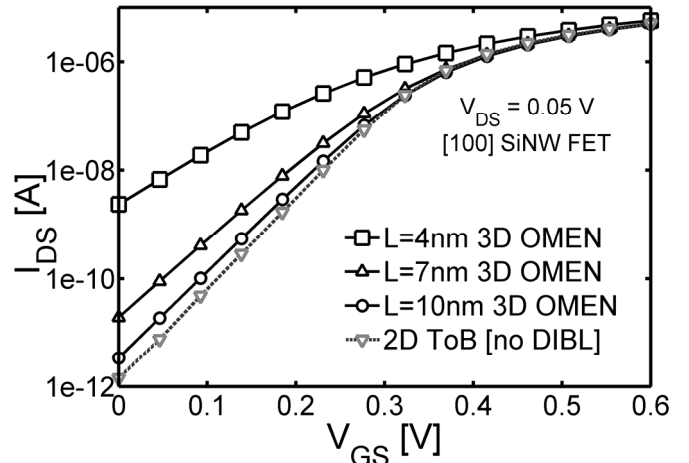


Figure 1.  $I_D$ - $V_G$  plot obtained for a  $3.1 \text{ nm} \times 3.1 \text{ nm}$ , [100] square SiNW with GAA oxide using 3D OMEN for different  $L_c$  and ToB (without DIBL adjustment). At  $L_c=10\text{nm}$ , results from 2 methods are in close agreement.

width. Finally we also provide a rule of thumb for the valid simulation domain for SiNW FET devices where ToB model can be used faithfully. We also provide a comparison of compute times for the full 3D and the 2D ToB model.

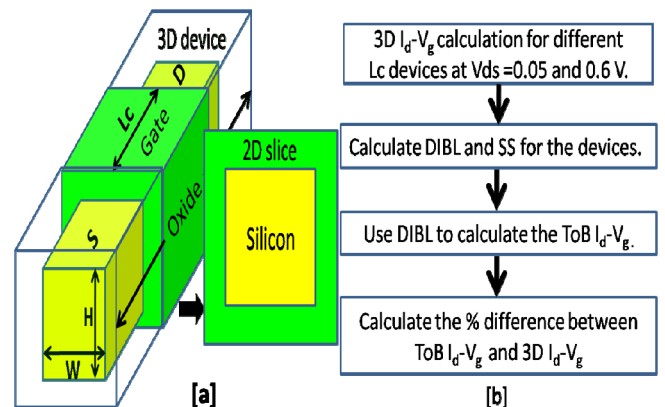


Figure 2. (a) 3D GAA SiNW MOSFET.  $L_c$  shows the gate/channel length. A 2D slice (one unitcell long) from this part is taken for ToB simulation. S and D represent source and drain respectively. W and H are silicon body width and height respectively. (b) Flowchart showing the numerical simulation approach used in this work.

## II. APPROACH

*Simulation Procedure:* First a full 3D atomistic ballistic simulation [9, 10, 11, 16, 17, 18] is performed for gate-all-around (GAA) rectangular n-type SiNW FETs with a given cross-section width (W) and height (H), keeping  $W/H = 1$ , (Fig.2a) using OMEN [17, 18] for different gate lengths ( $L_c$ ). The channel orientation is also specified for the FETs. 3D  $I_D$ - $V_G$  simulations are done for low and high drain biases ( $V_{DS}$ ). From these  $I_D$ - $V_G$  curves DIBL is extracted. Using this DIBL value 2D  $I_D$ - $V_G$  are simulated for exactly the same devices, using the ToB model to account for different ‘channel lengths’ (Fig. 2b).

*Simulation environment and devices:* Square silicon nanowire FETs with cross-section size of 3.1 nm (W)  $\times$  3.1 nm (H) and  $T_{ox}$  of 2nm are simulated using the 3D model for two different drain biases of  $V_{DS} = 0.05V$  (low) and 0.6V (high). Different channel lengths of 4, 7, 10, and 15 nm have been simulated with [100] and [110] channel orientations. The source/drain extension is 10nm with  $1e20cm^{-3}$  n-type doping. Exactly the same device structures are then simulated using the 2D ToB model.

## III. RESULTS & DISCUSSION

*Source/Drain tunnelling current:* Figure 1 shows that  $I_D$ - $V_G$  from ToB is in good agreement with the 3D OMEN result at low  $V_{DS}$ , without any DIBL compensation, for  $L_c = 10nm$ . The deviation at shorter  $L_c$  can only be attributed to S/D tunnelling current [19, 20] under ballistic condition, which is not included in the ToB model. Fig.3a and table I shows that the sub-threshold swing (SS) becomes considerably larger than 60mV/dec (ideal ToB result) with decreasing  $L_c$  for both [100] & [110] SiNW, reflecting strong S/D tunnelling current in the OFF-state. Also [110] wires show larger SS compared to [100] wires [19], hence making them less scalable. Thus, increased S/D tunnelling current causes 2D ToB to deviate from 3D  $I_D$ - $V_G$  results for reduced  $L_c$  devices.

*Source to channel barrier ( $\phi_{sc}$ ):* Figure 4. and insets of Fig.5 and Fig.6 show that the source to channel barrier reduces as  $V_{GS}$  increases. This decrease is stronger for smaller  $L_c$

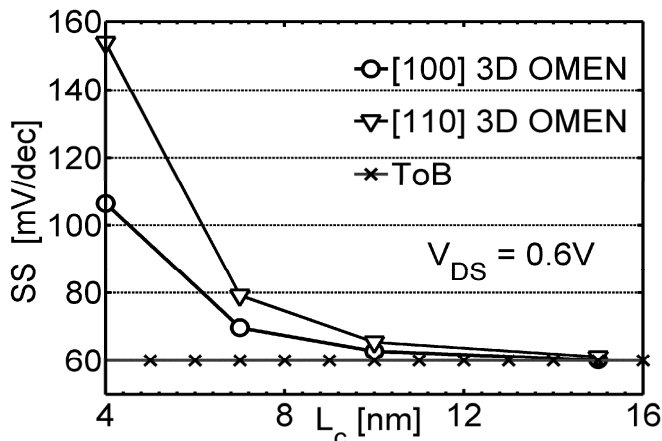


Figure 3. Sub-threshold swing (SS) for [100] and [110] SiNW FETs obtained from full 3D OMEN. ToB results in the ideal 60 mV/dec SS.

\*DIBT is Drain Induced Barrier Thinning

TABLE I. SHORT-CHANNEL CHARACTERISTICS (SCE) FOR  $\langle 100 \rangle$  AND  $\langle 110 \rangle$  ORIENTED SINW FETs OBTAINED FROM OMEN [3] AND THE VALID SIMULATION REGIME FOR ToB.

$L_c$ nm	SS (mV/dec)		DIBL(mV/V)		ToB valid	
	100	110	100	110	100	110
4	106.4	158.2	175.4	201.2	No	No
7	69.71	80.1	70.92	80.27	No	No
10	62.80	63.6	11.58	13.69	Partly	Partly
15	60.19	60.89	4.17	4.04	Yes	Yes

devices (Fig.4). ToB shows a strong deviation from 3D  $I_D$ - $V_G$  results since the source to channel barrier becomes much smaller than the  $KT/q$  limit and causes an excessive S/D tunnelling current to flow. Thus, existence of proper source to channel barrier is important for ToB to match 3D results.

*Longer  $L_c$  devices:* To obtain the device regime where ToB provides reliable results, it is important to understand the effect of gate and drain electrostatics on the source to channel barrier. Figure 5 shows that ToB provides good agreement to 3D results for  $L_c = 15nm$  (long channel) in the OFF-state since the S/D barrier is well defined at low  $V_{GS}$  & high  $V_{DS}$  and also the tunnelling current is minimal due to longer  $L_c$ . However, in the ON-state ToB current is smaller compared to 3D under high  $V_{GS}$  and  $V_{DS}$ . As  $V_{GS}$  increases, the S/D barrier decreases, as a result carriers injected at the source side are no more reflected by the barrier. To ensure charge neutrality in the source, the electrostatic potential on the source side ( $\phi_{sc}$ ) decreases allowing more carrier injection causing an artificial increase in the ON-current. This is an artifact of the ballistic approximation that is not captured in ToB model and explains why the full 3D OMEN ON-current is larger at high  $V_{GS}$  (Fig.5 & 6)

*Shorter  $L_c$  devices:* As  $L_c$  decreases the drain bias starts to reduce the S/D barrier width (DIBT\*) [20] (Fig.6 inset) causing

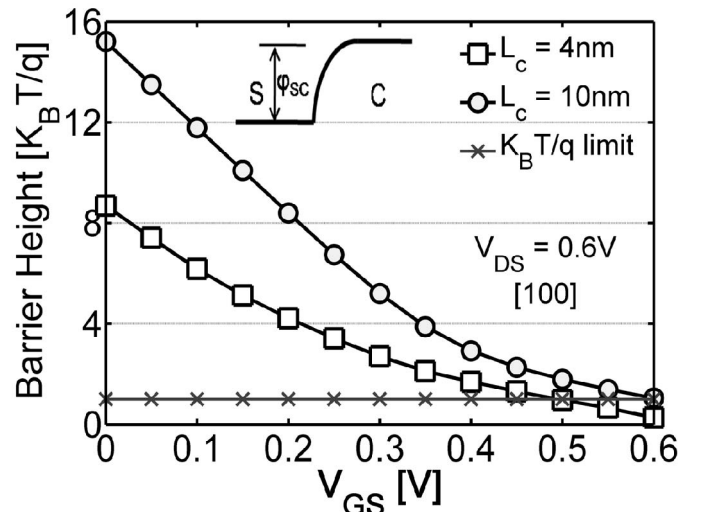


Figure 4. Source to channel barrier ( $\phi_{sc}$ ) height in terms of  $K_B T/q$  for [100] devices at two gate lengths. Inset shows the energy barrier between the source (S) and the channel (C).

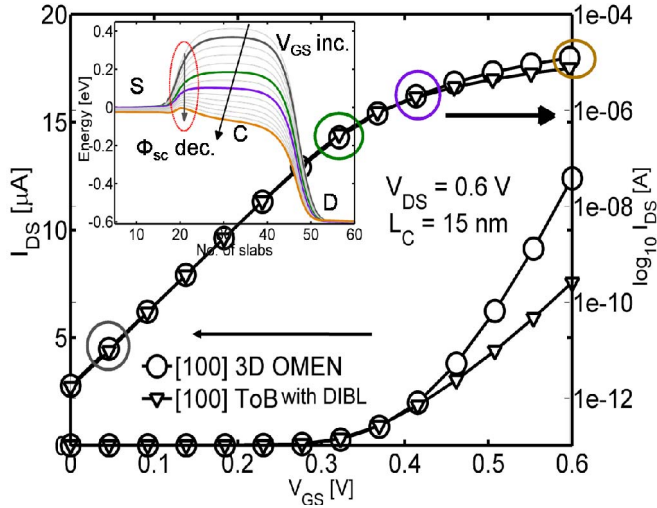


Figure 5. Long  $L_c$   $I_D$ - $V_G$  characteristics for ToB (with DIBL) vs. 3D OMEN for [100] SiNW,  $L_c = 15\text{nm}$ , at  $V_{DS} = 0.6\text{V}$ . Inset shows the variation in the S/D barrier at 4 different  $V_{GS}$  computed using 3D OMEN.  $I_{OFF}$  shows very good agreement; however,  $I_{ON}$  is higher for 3D.

excessive S/D tunnelling current to flow. For  $L_c = 4\text{nm}$  (short channel), ToB results are not in good agreement with full 3D OMEN anywhere (Fig.5) since the S/D barrier is not well defined and is below the thermal  $KT/q$  limit (Fig.4). Absence of a clear S/D barrier makes ToB inapplicable to short  $L_c$  devices. As a quantitative estimate for tunnelling current rate ( $R_{TUN}$ ) (in the OFF-state) eqn. 1 is used:

$$R_{TUN} = 100 \times (J_{3D} - J_{TOB}) / J_{3D} \quad \text{----} \quad (1)$$

where,  $J_{3D}$ ,  $J_{TOB}$  are currents from 3D and ToB simulations, respectively. Figure 7 shows that at  $I_{OFF}$ , tunnelling rate ( $R_{TUN}$ ) increases dramatically with decreasing  $L_c$ , with [110] devices showing worse short channel effects (SCE) compared to [100] devices [19].

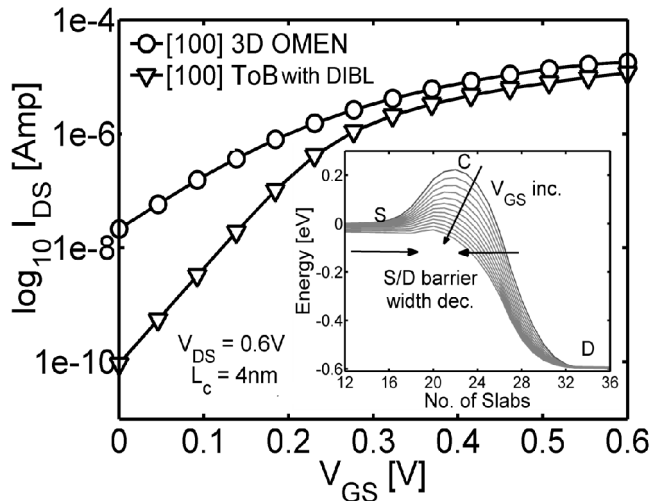


Figure 6. Short  $L_c$  comparison of  $I_D$ - $V_G$  from ToB (with DIBL) with 3D OMEN, for [100] SiNW FET,  $L_c=4\text{nm}$ . Inset shows the S/D barrier for the device which decreases in width and height as  $V_{GS}$  increases.

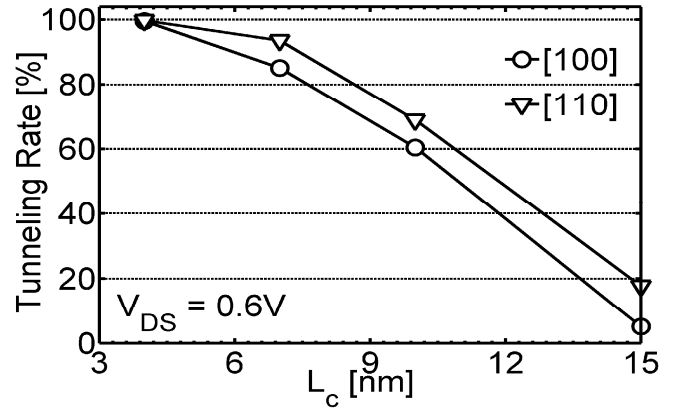


Figure 7. Tunneling current rate percentage in the off-state for [100] & [110] SiNW FETs for different  $L_c$ . Tunneling current decreases in OFF state, as  $L_c$  increases for both [100] and [110]. [110] wires have larger tunneling component hence worse short channel effect (SCE).

**Computational Speedup:** One advantage of using the ToB lies in the reduced compute time compared to the full 3D OMEN atomistic quantum transport simulation. For square ( $W/H = 1$ ) SiNW FETs, with longer  $L_c$  ( $L_c \gg 5*W$ ) devices 1 self-consistent Schrodinger-Poisson iteration time for 3D simulation goes as  $W^{n_{3D}}$ , with  $n_{3D} = 5.63$ , whereas for 2D ToB it goes as  $W^{n_{2D}}$ , with  $n_{2D} = 2.82$ , on a single CPU (Fig. 8).  $W$  is the silicon cross-section width (Fig.2a). The simulated devices have 1nm GAA oxide. Table II (next page) shows the actual compute times for both the models and the speedup obtained as a function of  $W$  for SiNW FETs. Speedup is defined by eqn.2.  $\lambda$  (eqn. 3) is the ratio of time intercepts for 3D and 2D simulation time (Fig. 8). Value of  $\lambda$  in Fig.8 is around 51. Speedup of 2D ToB simulations increases rapidly as  $W$  increases making it a very attractive model for device

$$\text{Speedup} = \lambda W^{(n_{3D} - n_{2D})} \quad \text{----} \quad (2)$$

$$\lambda = C_{3D}/C_{2D} \quad \text{----} \quad (3)$$

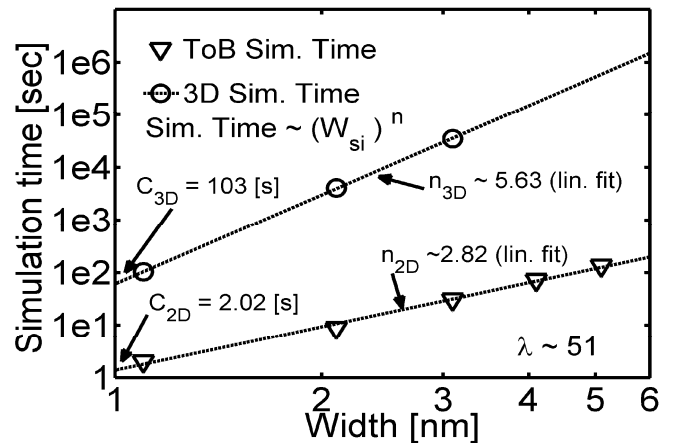


Figure 8. Simulation time for 1 self-consistent iteration for 3D OMEN vs. 2D ToB for a square SiNW with 1nm GAA oxide on 1CPU. ToB simulates  $\sim (W_{si})^2$  times faster compared to 3D OMEN, where  $W_{si}$  is the silicon body thickness.

TABLE II. COMPARISON OF ACTUAL SIMULATION TIME FOR FULL 3D AND 2D MODEL WITH SPEED-UP ACHIEVED FROM 2D ToB MODEL FOR DIFFERENT CROSS-SECTION WIDTH (W) SiNW FETs WITH 1NM GAA OXIDE.

W(width) [nm]	time[sec] (1 CPU)		Speed up ( $\lambda \sim 51$ )
	3D	2D	
1.1	103	2.02	66.65
2.1	4,080	8.92	410.13
3.1	35,200	30.63	1225.2
4.1	205,000	71.52	2688

simulation. Also the memory storage needed for ToB device simulation is much smaller compared to 3D simulation.

#### IV. CONCLUSION & OUTLOOK

Two factors are important in defining the valid device regime for ToB, (a) the presence of proper source to channel barrier ( $\phi_{sc} > KT/q$ ) and (b) a small source to drain tunneling current. Due to these reasons ToB compares well with 3D model for longer Lc devices. We find that for a ratio of Lc/W  $\geq 5$ , that the ToB model can be used to obtain accurate 3D results. ToB is a suitable model for SiNW FETs where channel electrostatics is controlled mostly by the gate. In this regime, DIBL from experiments can be fed to ToB, to obtain accurate terminal characteristics. Computational speedup (Table II) as well as smaller memory storage requirements makes ToB a very attractive model for typical device simulation. The ToB model provides significant insight into the importance of atomistic bandstructure effects in nanowires [13, 14]. [100] and [110] wire orientations show similar short channel effects (SCE) at sufficiently long channel lengths. Table 1 elucidates the SCE and the regimes where the ToB model is applicable. It is shown that [100] n-type SiNW FETs are more scalable compared to [110] wires (Table I). The full 3D OMEN transport model is now deployed on nanoHUB.org [18] and readers can duplicate our simulation results for small diameter silicon nanowire FETs. The ToB model used in this work is also released as a part of the existing Bandstructure Lab [21] on nanoHUB.org.

#### ACKNOWLEDGMENT

This work was supported by the Semiconductor Research Corporation (SRC), Microelectronics Advanced Research Corporation (MARCO) & Midwest Institute for Nanoelectronics Discovery (MIND). Computational resources were provided by [www.nanoHUB.org](http://www.nanoHUB.org), funded by National Science Foundation (NSF).

#### REFERENCES

[1] N. Singh et. al., "Ultra-narrow silicon nanowire gate-all-around CMOS devices: Impact of diameter, channel-orientation and low temperature on device performance," Int. Elec. Dev. Meeting, 2006.  
 [2] K. H. Cho, "Observation of single electron tunneling and ballistic transport in twin silicon nanowire MOSFETs (TSNWFETs) fabricated by top-down CMOS process," Int. Elec. Dev. Meeting, 2006.  
 [3] K. H. Cho, K.H. Yeo, Y.Y. Yeoh, S. D. Suk, M. Li, J. M. Lee, M.-S. Kim, D.-W. Kim, D. Park, B. H. Hong, Y. C. Jung, and S. W.

Hwang, "Experimental evidence of ballistic transport in cylindrical gate-all-around twin silicon nanowire metal-oxide semiconductor field-effect transistors," APL, 92, 052102, 2008.  
 [4] M. Kobayashi and T. Hiramoto, "Experimental study on quantum confinement effects in silicon nanowire metal-oxide-semiconductor field-effect transistors and single-electron transistors," J. Appl. Phys., 103, 053709, 2008.  
 [5] J. Xiang, W. Lu, Y. Hu, Y. Wu, H. Yan, and Charles M. Lieber, "Ge/Si nanowire heterostructures as high-performance field-effect transistors," Nature, vol. 441, no. 25, 2006.  
 [6] T. B. Boykin, G. Klimeck, and F. Oyafuso, "Valence band effective-mass expressions in the  $sp^3d^5s^*$  empirical tight-binding model applied to a Si and Ge parameterization," PRB, Vol. 69, pp. 115201-115210, 2004.  
 [7] N. Kharche, S. Kim, T. B. Boykin, and G. Klimeck, "Valley Degeneracies in (111) Silicon Quantum Wells", APL, Vol. 94, Issue 4, 042101, 2009.  
 [8] M.Usman, H. Ryu, I. Woo, D.S. Ebert, and G. Klimeck, "Moving towards nano-TCAD through multi-million atom quantum dot simulations matching experimental data", to appear in IEEE Transactions on Nanotechnology, 2009.  
 [9] M. Luisier, A. Schenk, W. Fichtner, and G. Klimeck, "Atomistic Simulation of Nanowire in the  $sp^3d^5s^*$  Tight-Binding Formalism: From Boundary Conditions to Strain Calculations", PRB 74, 205323, 2006.  
 [10] M.Luisier, and G. Klimeck, "Atomistic, Full-Band Design Study of InAs Band-to-Band Tunneling Field-Effect Transistors", accepted in IEEE EDL (2009).  
 [11] G. Klimeck and M. Luisier, "From NEMO1D and NEMO3D to OMEN: moving towards atomistic 3-D quantum transport in nano-scale semiconductors", Int. Elec. Dev. Meeting, 2008.  
 [12] Mathieu Luisier and Gerhard Klimeck, "A multi-level parallel simulation approach to electron transport in nano-scale transistors", Supercomputing 2008, Austin TX, Nov. 15-21, 2008  
 [13] N. Neophytou, A. Paul, M. Lundstrom and G. Klimeck, "Bandstructure Effects in Silicon Nanowire ElectronTransport", IEEE TED, Vol. 55, Issue 6, June 2008, 1286 - 1297.  
 [14] N. Neophytou, A. Paul, and G. Klimeck, "Bandstructure Effects in Silicon Nanowire Hole Transport", IEEE Transactions on Nanotechnology, Vol. 7, 710 - 719 (2008).  
 [15] N. Neophytou and G. Klimeck, "Design space for low sensitivity to size variations in [110] PMOS nanowire devices: The implications of anisotropy in the quantization mass", Nano letters Vol. 9 (2), pp 623-630 (2009).  
 [16] A. Rahman, J. Guo, S. Datta, and M. Lundstrom, "Theory of ballistic nanotransistors," IEEE Trans. Electron Devices, Vol. 50, no. 9, pp. 1853-1864, 2003.  
 [17] M. Luisier and G. Klimeck, "OMEN an atomistic and full-band quantum transport simulator for post-CMOS nanodevices", 8th IEEE Conf. On Nanotechnology, 2008, 354 - 357.  
 [18] <http://nanohub.org/resources/5359>; S.G. Kim, M.Luisier, B.P. Haley, A Paul, S.R.Mehrotra and G. Klimeck (2008), "OMEN Nanowire," DOI: 10254/nanohub-r5359.4.  
 [19] M. Luisier, A. Schenk and W. Fichtner, "Full-band atomistic study of source-to-drain tunneling in Si nanowire transistors", SISPAD, Vienna, Austria (2007).  
 [20] J. Wang and M. Lundstrom, "Does source-to-drain tunneling limit the ultimate scaling of MOSFETs? ", IEDM 2002, pp. 707-710  
 [21] <http://nanohub.org/resources/bandstrlab>; A. Paul, M. Luisier, N. Neophytou, R Kim, M. McLennan; M.S. Lundstrom and G. Klimeck (2006), "Band Structure Lab," DOI: 10254/nanohub-r1308.6.